

Effect of Pd Surface Roughness on the Bonding Process and High Temperature Reliability of Au Ball Bonds

Y. HUANG,¹ H.J. KIM,^{1,3} M. MCCRACKEN,¹ G. VISWANATHAN,² F. PON,²
M. MAYER,¹ and Y.N. ZHOU¹

1.—Center of Advanced Materials Joining, University of Waterloo, Waterloo, ON, Canada.
2.—NAND Solutions Group, Intel Corporation, Folsom, CA, USA. 3.—e-mail: kim.hyounghoon@gmail.com

A 0.3- μm -thick electrolytic Pd layer was plated on 1 μm of electroless Ni on 1 mm-thick polished and roughened Cu substrates with roughness values (R_a) of 0.08 μm and 0.5 μm , respectively. The rough substrates were produced with sand-blasting. Au wire bonding on the Ni/Pd surface was optimized, and the electrical reliability was investigated under a high temperature storage test (HTST) during 800 h at 250°C by measuring the ball bond contact resistance, R_c . The average value of R_c of optimized ball bonds on the rough substrate was 1.96 m Ω which was about 40.0% higher than that on the smooth substrate. The initial bondability increased for the rougher surface, so that only half of the original ultrasonic level was required, but the reliability was not affected by surface roughness. For both substrate types, HTST caused bond healing, reducing the average R_c by about 21% and 27%, respectively. Au diffusion into the Pd layer was observed in scanning transmission electron microscopy/energy dispersive spectroscopy (STEM-EDS) line-scan analysis after HTST. It is considered that diffusion of Au or interdiffusion between Au and Pd can provide chemically strong bonding during HTST. This is supported by the R_c decrease measured as the aging time increased. Cu migration was indicated in the STEM-EDS analysis, but its effect on reliability can be ignored. Au and Pd tend to form a complete solid solution at the interface and can provide reliable interconnection for high temperature (250°C) applications.

Key words: Au wire bonding, Ni/Pd finish, Au/Pd bonding, thermal aging, high temperature, reliability, *in situ* contact resistance

INTRODUCTION

Wire bonding continues to occupy about 90% of first-level chip interconnection due to its cost effectiveness and technological maturity.^{1,2} The standard Au wire bonding process on Al bond pads provides excellent initial bondability, but the Au/Al interface deteriorates due to the formation of brittle intermetallic compounds (IMCs) under high temperature storage conditions.^{2,3} Kirkendall voids accompanied with IMCs form at the Au/IMC interface and coalesce together into cracks. Finally, the Au/Al bonding interface becomes weakened by the

formation of brittle IMCs, cracks, and oxide. To avoid the degradation of the wire bonding interface induced by IMCs, new pad materials or final metal finishes for printed circuit boards (PCBs) are required.

A Ni/Pd metal finish was introduced by Texas Instruments in 1989 and has been widely used for leadframe, PCB, and automotive packaging.^{4,5} The driving forces of Pd finish are to replace expensive Pb-containing surface finish processes, such as hot air solder leveling, and to support fine pitch applications. The final Pd layer prevents oxidation of the Ni layer and provides good wire-bondability as well as solderability. Some researchers have reported results of bond reliability of Au ball bonding on Ni/Pd-capped Cu pads. The bonding interface was

(Received June 17, 2010; accepted February 16, 2011;
published online March 3, 2011)

reliable because of the complete solid solution between Au and Pd and the absence of IMC.^{6,7} However, the tested temperatures of the high temperature storage test (HTST) in those studies were less than 175°C, so that Au/Pd bond reliability at much higher temperature remains in doubt.

We investigated the reliability of Au wire bonding on Cu/Ni/Pd surface with the HTST at 250°C. Cross-sectioning, as a destructive test, was used to examine the bonding interface, and contact resistance (R_c) was monitored during the HTST period as a nondestructive test.

EXPERIMENTAL PROCEDURES

Test Substrate Preparation

The 500 μm -thick oxygen-free high thermal conductivity Cu sheet was precut to dimensions of 10 mm \times 10 mm. To compare the effect of surface roughness, all as-received Cu sheets were polished to reduce the average roughness (R_a) to 0.08 μm . One group of polished Cu sheets was kept as such, whereas another group was sand-blasted with fine bead at 20 psi for 5 s to generate an R_a of 0.5 μm , which was acceptable for bonding.⁸ Images of the surface morphology of both substrates are shown in Fig. 1. All samples were rinsed with ethanol in an ultrasound bath and completely dried before plating.

Ni and Pd Plating

Standardized electroless Ni (EL-Ni) plating on Cu was employed with target thickness of 1 μm . Before plating, the Cu substrate was air-brushed to remove dirt from the surface. Cleaning agents were used to

minimize the grease and oxidation on the Cu surface at room temperature. During the EL-Ni plating, a potential difference was generated between the steel clip and Cu substrate for 15 s to initiate the plating process. The deposition time for Ni was optimized to about 150 s. For optimal quality and consistency of film thickness, the substrate was placed horizontally in the solution, while the clips used for handling the substrate were placed as close to the edge of the substrate as possible.

An industrial electrolytic Pd (E-Pd) plating setup was used for 0.3 μm target thickness. A constant current was applied to supply the potential difference during the plating process. The deposition time for Pd was about 50 s. The substrate was placed vertically in the beaker, with the surface to be plated directly facing the anode to maximize the electromagnetic field for optimum plating quality. Periodic replenishment of the bath is required to avoid contamination over long periods of time. Ammonium hydroxide and hydrochloric acid were used to increase and decrease the pH, respectively, during the plating process. After plating, the substrates were rinsed with deionized water and blow-dried by air gun. The chemical concentrations of the plating baths were as recommended by the suppliers.

Wire Bonding

An ESEC 3088 automatic wire bonder (ESEC, Cham, Switzerland) with ultrasound frequency of 130 kHz was used for bonding of 4 N (99.99%) Au wire supplied by MKE Co. Ltd., Yongin, South Korea. Both ball and wedge bonds were formed on the Cu/Ni/Pd test substrate. Wire bonding

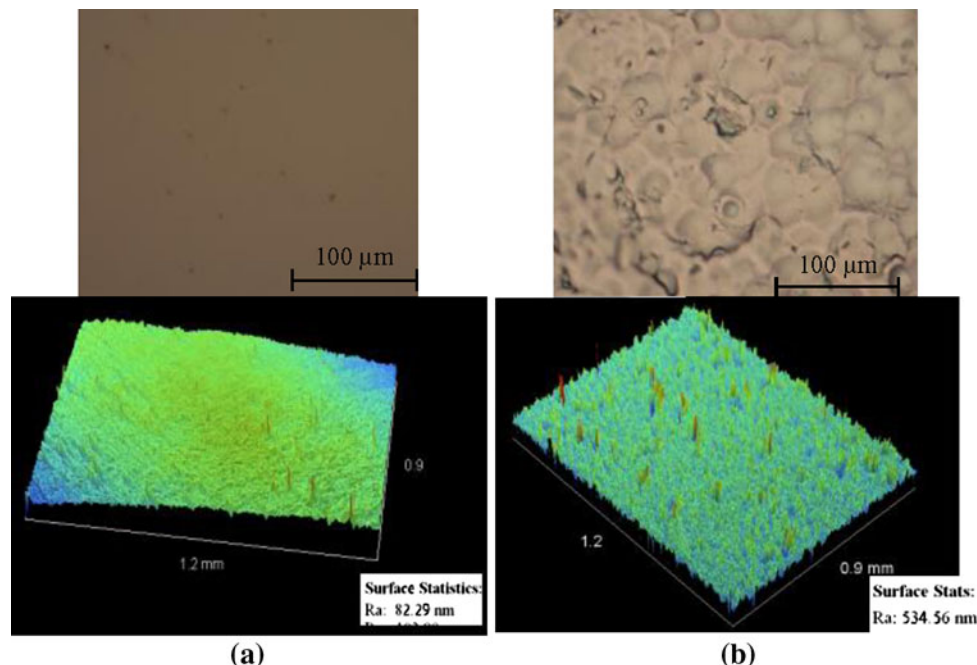


Fig. 1. Surface morphologies of (a) smooth substrate ($R_a = 0.08 \mu\text{m}$) and (b) rough substrate ($R_a = 0.5 \mu\text{m}$).

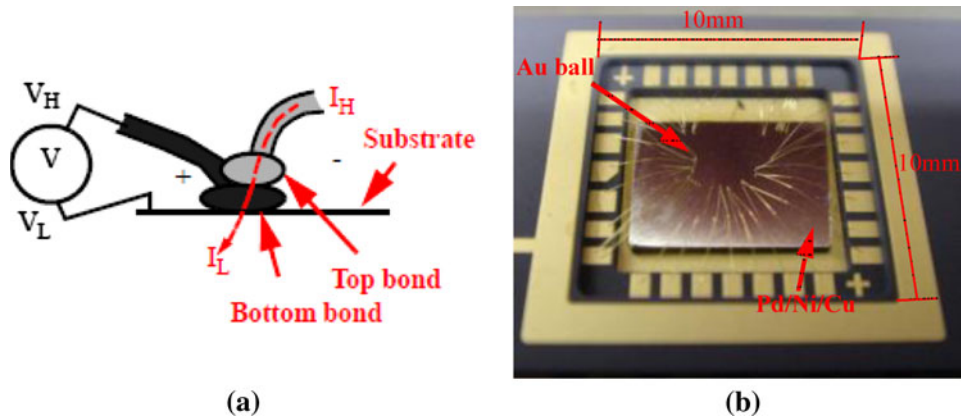


Fig. 2. (a) Schematics of R_c measurement with the four-point resistance method, and (b) 28-pin DIP after wire bonding for *in situ* R_c measurement.

parameters were optimized in terms of mashed ball diameter, mashed ball height, and shear strength (SS). The optimized wire bonding parameters, such as impact force, bonding force, and bonding time, were the same for the two substrates with different roughness except that the ultrasonic amplitude (US) optimized for the rougher substrate was 18% of US, being half of that optimized for the smoother substrate (36% of US).

High Temperature Storage Test

After the wire bonding process, both groups of test substrates were placed in an oven to conduct the HTST. The test substrates were thermally aged at 250°C up to 200 h and cross-sectioned to observe the change at the Au/Pd bonding interface. *In situ* measurement of R_c was monitored up to 800 h of thermal aging.

Microstructural Investigation

The specimens were mounted in epoxy. Fine polishing was performed up to 0.05 μm diamond suspension, and the polished samples were cleaned with ethanol and dried. The bonding interface between Au and Pd was observed by using a LEO field emission scanning electron microscope (FE-SEM) 1530. A JEOL 2010 field emission transmission electron microscope/scanning transmission electron microscope (FE-TEM/STEM) was used to further characterize the Au/Pd bonding interface. In STEM mode, its spot size has been optimized to 1 nm. This allows for high magnification imaging and energy dispersive spectroscopy (EDS) analysis of materials. The focused ion beam (FIB)-aided lift-off technique was adopted for TEM sampling, and the ion-milled TEM sample was attached to a Cu grid for investigation.

In Situ Contact Resistance (R_c) Measurement

The wire configuration for R_c measurement by the method of four-point resistance measurement is

illustrated in Fig. 2a. A second wire was attached to the first ball bond using a modified bonding parameter with a 90% reduced US parameter. Constant current of I_c was fed via the second wire through the ball bond, and at the same time, the voltage drop ($V_H - V_L$) was measured at the bonding interface. R_c was calculated by using Ohm's law. The four-wire configuration improves the accuracy of the final resistance reading by eliminating the wire span resistance from the measurement.⁹

As shown in Fig. 2b, a 28-pin dual in-line package (DIP) was used for attaching the plated specimen. Twenty-six pins of the DIP were used to bond 13 sets of double bonds, with each set corresponding to V_H (bottom bond) and I_H (top bond). A maximum of 13 R_c measurements can be generated from one DIP. The remaining two pins V_L and I_L were for the substrate.

The connection diagram for *in situ* R_c measurement during thermal aging is shown in Fig. 3. The multiplexer was used in combination with customized software on a computer to switch between the 13 bonds and record the resistance readings from each sample via a nanovoltmeter (Agilent 34420A). The nanovoltmeter was used in four-point resistance measurement mode, supplying constant current of $I_c = 0.1$ mA. The surrounding temperature was measured by a Pt100 resistive temperature detector. Along with the samples for R_c measurement, the Pt100 unit was placed inside the oven, and the resistance was recorded using a data acquisition unit connected to a computer. During the HTST, the temperature was maintained in the range $250 \pm 0.49^\circ\text{C}$.

RESULTS AND DISCUSSION

SS of As-Bonded Samples

As described previously and shown in Fig. 4, lower US was required for the rougher surface ($R_a = 0.5$ μm) substrate, resulting in an about 3.1% higher average ball SS with less deviation. Thus,

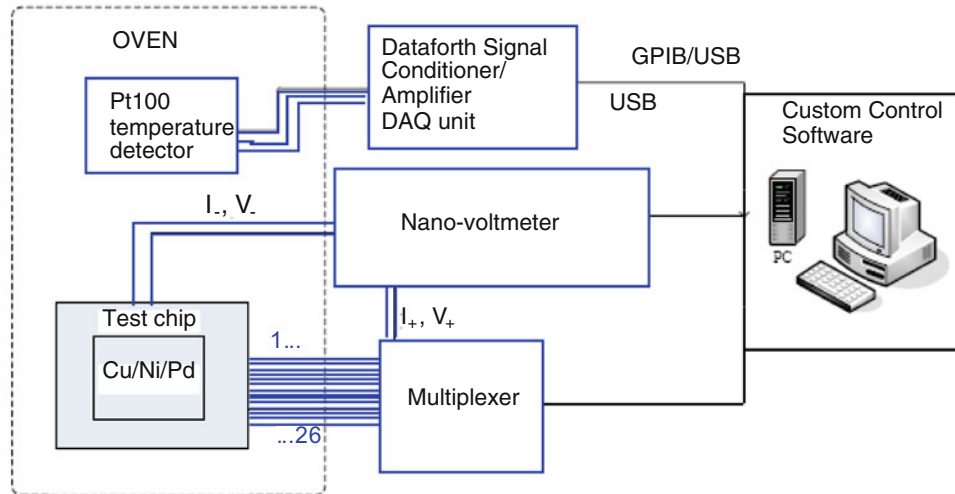


Fig. 3. Connection diagram for R_c measurement of Au ball bonds to Cu/Ni/Pd substrate during HTST.

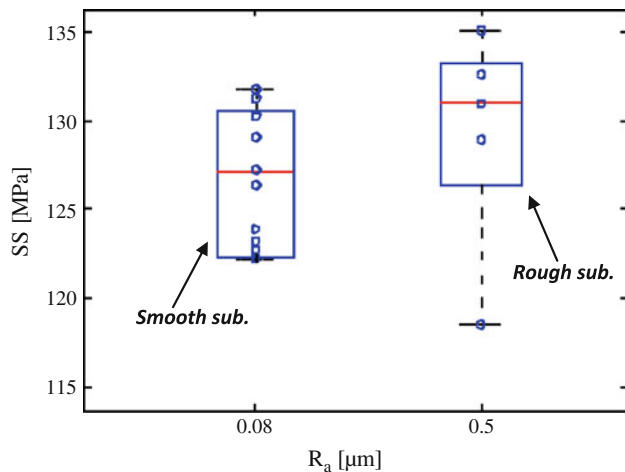


Fig. 4. As-bonded Au ball bond SS with different substrate surface roughnesses.

surface roughness ($0.5 \mu\text{m}$ in this study) can assist the action of ultrasound during wire bonding and enhance the bonding strength. In addition, interdiffusion and IMC formation are negligible in the as-bonded state. It can be considered that the higher SS of the rougher substrate is probably due to mechanical interlocking or higher friction power densities, localized at asperities.

Au/Pd Bonding Interface Observation

Figure 5a–d shows SEM micrographs of Au/Pd bonding interfaces from the as-bonded state up to thermally aged for 200 h. Each metallic layer can be easily distinguished by the high contrast of the back-scattered electron imaging mode and is labeled in the figures. According to the SEM images of Fig. 5, there is no notable interfacial change at the Au/Pd bonding area between as-bonded and

long-term aged substrates. It can be considered that Au and Pd do not form IMCs or voids even after 200 h of thermal aging at 250°C . This corresponds to the binary Au-Pd system, where Au and Pd show complete solid solution in the whole composition range. Previous studies that performed HTST of Au/Pd bonding at less than 175°C reported no IMC formation after thermal aging.^{7,10} However, the effect of smearing during polishing sometimes limits the accuracy of SEM results. Therefore, TEM analysis was performed for further investigation.

An FIB-aided lift-off technique was used to prepare the TEM sample. Figures 6 and 7 show the results of x-ray line-scan of the Cu, Ni, Pd, and Au metallic layer in the STEM-EDS mode. For the clear understanding of compositional changes, the profiles of each element are depicted separately on the right-hand side of both figures. In Fig. 6, there is a significant Cu presence across the interface, and the amount of Cu is dominant especially in the Au region. The line-scan at the Au/Pd bonding interface was performed including O in addition to 4 metal elements (see Fig. 7). The line-scan signal of O in the system is negligible compared with that of the other elements. Similar to Fig. 6, the amount of Cu increases in the Au region. Two possible causes can be considered for the presence of Cu in the Au region. One is pre-existing Cu atoms that diffused out through the Ni/Pd layer at room temperature before wire bonding, and the other is Cu migration that occurred during thermal aging. The pre-existing Cu can easily oxidize when the substrate is exposed to high temperature during wire bonding, and the Cu oxide deteriorates the bondability. This means that oxygen atoms in Cu oxide should be detected in the STEM-EDS line-scan, but the amount of oxygen was negligible. Therefore, the presence of Cu in the Au region is probably due to Cu migration through the Ni/Pd layer at 250°C .

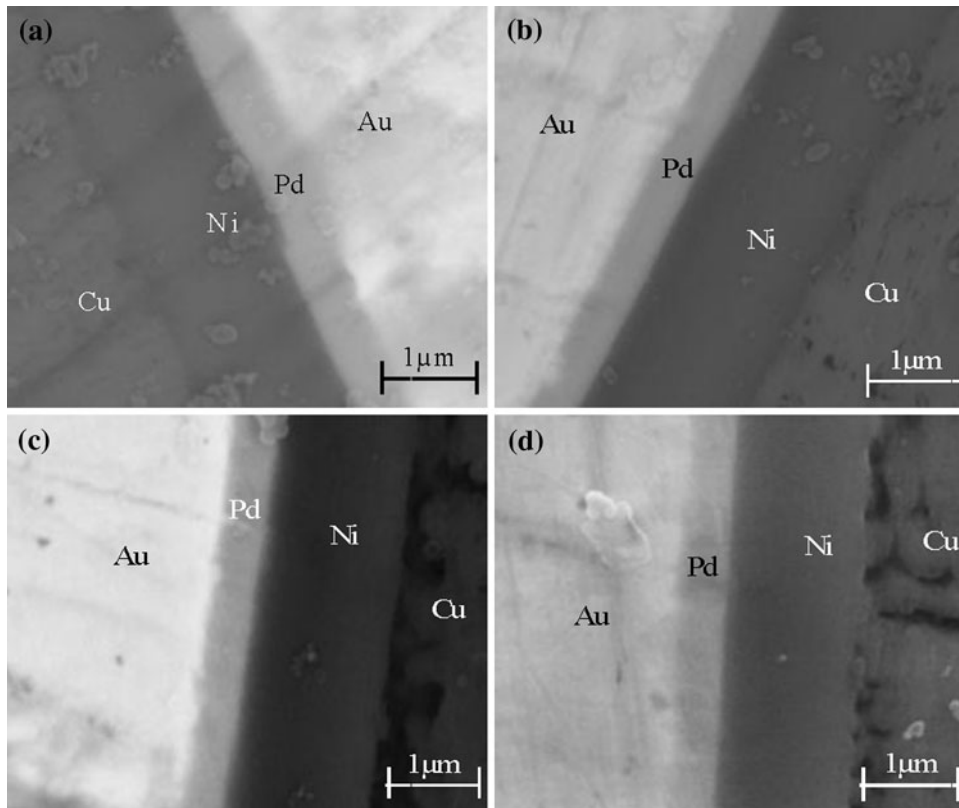


Fig. 5. SEM micrographs of bonding interfaces of (a) as-bonded substrate, and substrates thermally aged for (b) 50 h, (c) 100 h, and (d) 200 h.

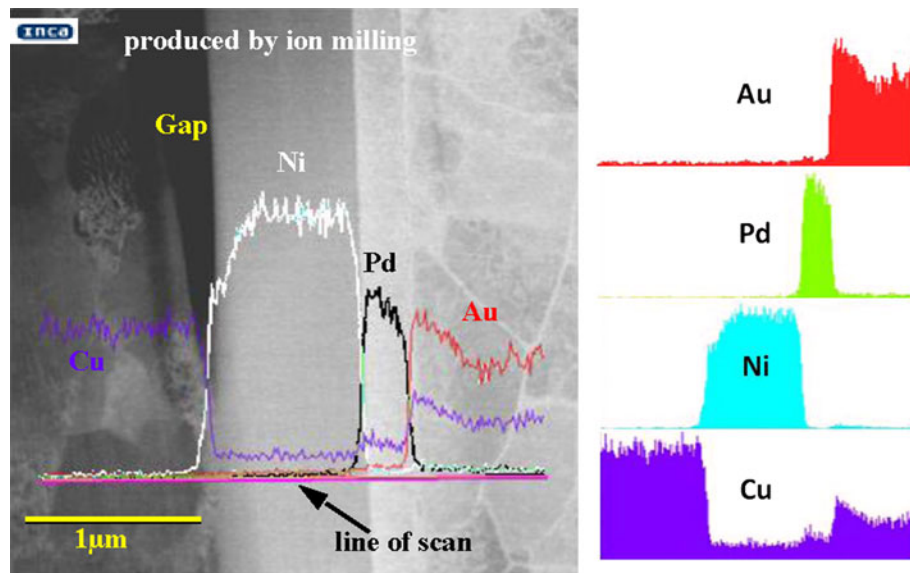


Fig. 6. STEM-EDS line-scan across the Cu/Ni/Pd/Au interface, thermally aged at 250°C for 200 h.

Sasangka and Tan⁶ reported a similar Cu migration phenomenon under thermal aging conditions of 150°C and 175°C. According to their results, Cu migration was observed when they used a 1 μm -thick Ni layer. It did not affect the bond reliability after thermal aging at 150°C and 175°C up to 1008 h. The TEM results confirm the lack of IMC as

reported, e.g., by Ratchev et al.¹⁰ for Au ball bonds on a Ni/Pd/Au surface aged at 150°C over 120 days. As shown in Figs. 6 and 7, there is no evidence of IMC formation at the Au/Pd interface. Poate et al.¹¹ reported that there was approximately 0.3 at.% Au diffused into Pd with about 0.5 μm depth, and that substantial Pd diffused into Au at a temperature of

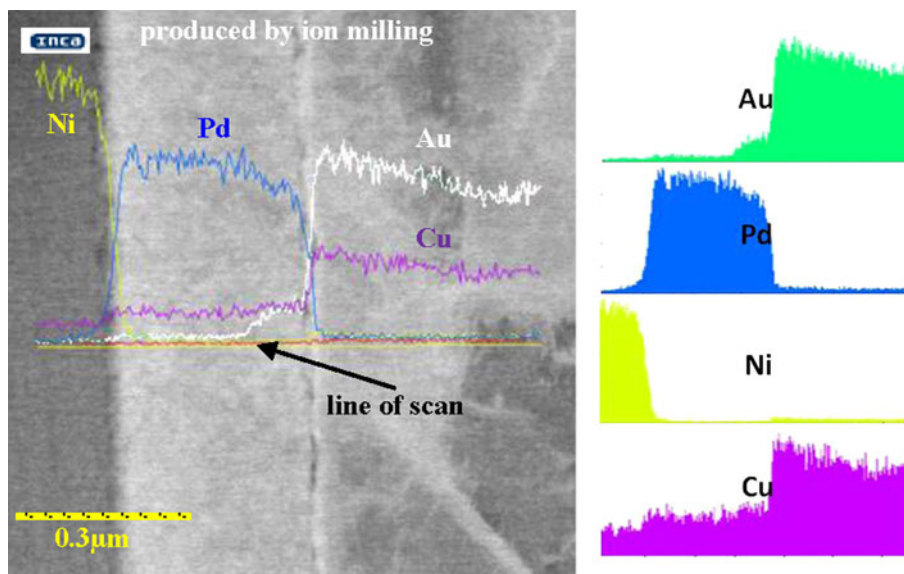


Fig. 7. STEM-EDS line-scan focused on the Au/Pd interface, thermally aged at 250°C for 200 h.

250°C over 2 h. Similarly, diffused Au atoms in Pd were detected, but there were no interfacial defects, such as voids, IMC, and crack formation, induced by the interdiffusion. Consequently, Au ball bonding on a Pd layer provides a robust bonding interface under thermal aging at 250°C.

In Situ Contact Resistance Measurement

For *in situ* temperature measurement during HTST, a Pt100 sensor was placed in the oven during the whole HTST. The resistance data of the Pt100 were recorded during HTST, and the values were converted to temperature by using

$$R_{\text{Pt100}} = 100 \Omega(1 + aT + bT^2), \quad (1)$$

where $a = 3.9083 \times 10^{-3} \text{ K}^{-1}$ and $b = -5.775 \times 10^{-7} \text{ K}^{-2}$ are constants.

Initial resistance measurements were measured as reference values at room temperature before starting the HTST by directly connecting to the multimeter (bypassing the multiplexer). Same measurements were then repeated with the samples connected to the multiplexer. The two results were identical, which indicates that the multiplexer does not add any offset to the R_c measurements. After 1 h of measurements at room temperature, the oven was reprogrammed to 50°C and 100°C, each for 30 min. Results from these additional temperature levels were used to calculate the temperature coefficient (TC) of the R_c ,

$$\text{TC}(T) = \frac{dR/dT}{R_c(T)}, \quad (2)$$

where T is the temperature and $R_c(T)$ is the contact resistance at T . The average TC at 20°C was 0.0022 K^{-1} , and it was independent of temperature

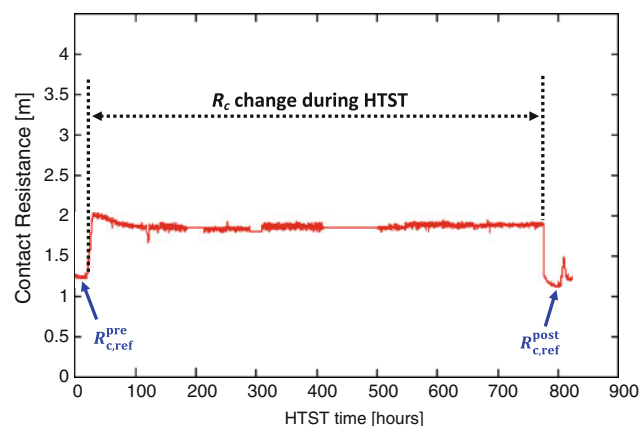


Fig. 8. Typical curve of *in situ* R_c measurement during HTST at 250°C.

change. Therefore, the value $R_{c,\text{ref}} = R_c(T_{\text{ref}})$ serves as a reference value between the R_c results before and after aging. The reference temperature, T_{ref} , was set at 20°C ($T_{\text{ref}} = 20^\circ\text{C}$), and the reference resistances of the both substrates before ($R_{c,\text{ref}}^{\text{pre}}$) and after aging ($R_{c,\text{ref}}^{\text{post}}$) were measured at 20°C.

Figure 8 shows the typical behavior of *in situ* R_c measurement during HTST, and the measurement points of $R_{c,\text{ref}}^{\text{pre}}$ and $R_{c,\text{ref}}^{\text{post}}$. R_c increased during heating from room temperature to 250°C and then decreased slightly before stabilizing during aging. The reference resistances of the smooth substrate before ($R_{c,\text{ref}}^{\text{pre}}$) and after ($R_{c,\text{ref}}^{\text{post}}$) aging are presented in Table I. We were able to obtain stable R_c signals from 10 double bonds that formed on the smooth substrate. In comparisons of the reference resistances before and after HTST for 800 h at 250°C, 9 double bonds showed $R_{c,\text{ref}}^{\text{pre}} \geq R_{c,\text{ref}}^{\text{post}}$. The reference resistances of the rough substrate are listed in

Table I. Comparison of R_c values before and after HTST for the smooth substrate ($R_a = 0.08 \mu\text{m}$)

Ball Bond	Before Aging $R_{c,\text{ref}}^{\text{pre}}$ (m Ω)	After Aging $R_{c,\text{ref}}^{\text{post}}$ (m Ω)	Difference (%)
1	1.7	1.4	-17.65
2	1.4	1.3	-7.14
3	1.1	1	-9.09
4	1.1	1	-9.09
5	1.4	1.2	-14.29
6	1.4	1.3	-7.14
7	0.5	1	100
8	1.2	1.1	-8.33
9	2.2	1.8	-18.18
10	2	1.3	-35
Average	1.40 ± 0.49	1.24 ± 0.25	-21.05

Table II. Comparison of R_c values before and after HTST for the rough substrate ($R_a = 0.5 \mu\text{m}$)

Ball Bond	Before Aging $R_{c,\text{ref}}^{\text{pre}}$ (m Ω)	After Aging $R_{c,\text{ref}}^{\text{post}}$ (m Ω)	Difference (%)
1	1.6	1.5	-6.25
2	1.8	1.8	0
3	1.6	1.6	0
4	1.8	1.5	-16.67
5	1.4	1.3	-7.14
6	2.1	2.0	-4.76
7	5.6	1.9	-66.07
8	1.0	0.9	-10
9	1.3	1.1	-15.38
10	1.7	1.6	-5.88
11	1.7	1.7	0
Average	1.96 ± 1.24	1.54 ± 0.33	-27.27

Table II. The average $R_{c,\text{ref}}$ values were calculated from the 11 double bonds that showed stable R_c signals. The average $R_{c,\text{ref}}^{\text{pre}}$ and $R_{c,\text{ref}}^{\text{post}}$ values of the rough substrate were 40.0% and 24.2% higher, respectively, than those of the smooth substrate, but the tendencies of R_c decrease after HTST were similar. Interestingly, in contrast to Au-Al bonds which deteriorate during HTST, the Au-Pd bonds observed here showed excellent robustness.

Logie et al.¹² reported an increase in resistivity from pure Au or Pd to AuPd alloys at liquid-nitrogen temperature. To correlate these results with the experiments conducted, if Au/Pd IMC formed at the bonding interface, R_c would be expected to increase similarly to that in Ref. ¹². As R_c did not increase during aging, it can be considered that little or no Au/Pd IMC formed at the bond interface. The negligible variation of TC between pre- and post-aging also reconfirms the lack of substantial IMC. Although no IMC formed at the bonding interface, Au and Pd interdiffusion can occur. Au diffusion into Pd was indicated by the result of the STEM-EDS line-scan. As shown in the Au-Pd

binary phase diagram, Au and Pd form a complete solid-solution phase, the resistance of which may slightly increase with changing composition, so that higher $R_{c,\text{ref}}^{\text{post}}$ can be supposed than $R_{c,\text{ref}}^{\text{pre}}$. However, R_c decreased after thermal aging. Micron- or sub-micron-size interfacial gaps inevitably remain after most wire bonding processes, increasing R_c above its theoretical minimum. It can be easily confirmed that the rougher substrate showed the higher initial R_c . During thermal aging at high temperature, Au and Pd atoms are diffusing actively not only inside grains or at grain boundaries, but also at surfaces. Therefore, diffusion can fill the interfacial gaps and metallurgically connect mechanically unbonded areas during HTST. Such an increase of actual bonding area reduces the R_c value. Another possible mechanism affecting R_c is thermal annealing of the metals, where recovery of dislocations generated in the Au ball bonding process takes place.¹³ The average R_c decreased by about 23.9% and 20.7% for the 0.08 μm and 0.5 μm roughness substrates after HTST, respectively.

The Ni/Pd finish on Cu provided excellent bond reliability for Au wire, and the effect of Cu migration on reliability was negligible. This indicates that Pd finish is a candidate to replace the conventional Al pad for high temperature applications.

CONCLUSIONS

A relatively rough surface was found to be beneficial for bondability of Au on Pd by reducing the ultrasound required to achieve a high-quality bond by 50%, probably due to the locally increased mechanical friction power density at the bonding interface. Reduced ultrasound results in reduced average stresses under the pad during bonding, reducing the risk of underpad damage. Therefore, increasing the bonding pad roughness can be beneficial for Au ball bonding robust to underpad damage. Even after thermal aging at 250°C, Au wire bonding on the Pd layer showed a robust bonding interface without any void or IMC formation, resulting in highly stable electrical continuity. Au and Pd interdiffuse and form a complete solid-solution phase, which might contribute to the enhancement of contact resistance. Therefore, Au wire bonding on a Pd layer is a good candidate for high temperature applications, and further evaluation of bond stability above 250°C is recommended.

ACKNOWLEDGEMENTS

The authors would like to thank Intel Corporation, Folsom, CA, USA for financial support.

REFERENCES

1. N. Srikanth, S. Murali, Y.M. Wong, and C.J. Vath III, *Thin Solid Films* 462–463, 339 (2004).
2. G. Harman, *Wire Bonding in Microelectronics*, 3rd ed. (New York: McGraw-Hill Professional, 2010).
3. A. Karpel, G. Gur, Z. Atzmon, and W.D. Kaplan, *J. Mater. Sci.* 42, 2347 (2007).

4. D.C. Abbott, *IEEE Trans. Compon. Packag. Technol.* 22, 99 (1999).
5. C. Fan, J.A. Abys, and A. Blair, *Circuit World* 25, 23 (1999).
6. W.A. Sasangka and A.C. Tan, *Proceedings of the Electronic Packaging Technology Conference* (2006), p. 330.
7. TN-29-24: Micron Wire-Bonding Techniques Overview, Technical Note, Micron, 1, 2006.
8. M. Pecht, *Handbook of Electronic Package Design* (New York: CRC Press, 1991).
9. M. Mayer, *Proceedings of the Electronic Components and Technology Conference* (2008), p. 1762.
10. P. Ratchev, S. Stoukatch, and B. Swinnen, *Microelectron. Reliab.* 46, 1315 (2006).
11. J.M. Poate, P.A. Turner, and W.J. DeBonte, *J. Appl. Phys.* 46, 4275 (1975).
12. H.J. Logie, J. Jackson, J.C. Anderson, and F.R.N. Nabarro, *Acta Metall. Mater.* 9, 707 (1996).
13. C.V. Kopetskii, G.I. Kulesko, L.S. Kokhanchik, and O.V. Zharikov, *Phys. Status Solidi A* 22, 185 (1974).